EBioMedicine 38 (2018) 248–256

Contents lists available at ScienceDirect

EBioMedicine

journal homepage: www.ebiomedicine.com

EBioMedicine
Published by THE LANCET

Research paper

Protease activity sensors noninvasively classify bacterial infections and antibiotic responses

Colin G. Buss [a,b,1], Jaideep S. Dudani [a,c,1], Reid T.K. Akana [c], Heather E. Fleming [a,b], Sangeeta N. Bhatia [a,b,d,e,f,g,*]

[a] Koch Institute for Integrative Cancer Research, Massachusetts Institute of Technology, Cambridge, MA 02139, USA
[b] Harvard–MIT Health Sciences and Technology Program, Institute for Medical Engineering and Science, Massachusetts Institute of Technology, Cambridge, MA 02139, USA
[c] Department of Biological Engineering, Massachusetts Institute of Technology, Cambridge, MA 02139, USA
[d] Department of Electrical Engineering and Computer Science, Massachusetts Institute of Technology, Cambridge, MA 02139, USA
[e] Department of Medicine, Brigham and Women's Hospital, Harvard Medical School, Boston, MA 02115, USA
[f] Broad Institute of Massachusetts Institute of Technology and Harvard, Cambridge, MA 02139, USA
[g] Howard Hughes Medical Institute, Cambridge, MA 02139, USA

ARTICLE INFO

Article history:
Received 29 June 2018
Received in revised form 8 November 2018
Accepted 15 November 2018
Available online 29 November 2018

Keywords:
Protease
Nanoparticle
Diagnostic
Bacterial pneumonia

ABSTRACT

Background: Respiratory tract infections represent a significant public health risk, and timely and accurate detection of bacterial infections facilitates rapid therapeutic intervention. Furthermore, monitoring the progression of infections after intervention enables 'course correction' in cases where initial treatments are ineffective, avoiding unnecessary drug dosing that can contribute to antibiotic resistance. However, current diagnostic and monitoring techniques rely on non-specific or slow readouts, such as radiographic imaging and sputum cultures, which fail to specifically identify bacterial infections and take several days to identify optimal antibiotic treatments.
Methods: Here we describe a nanoparticle system that detects *P. aeruginosa* lung infections by sensing host and bacterial protease activity *in vivo*, and that delivers a urinary detection readout. One protease sensor is comprised of a peptide substrate for the *P. aeruginosa* protease LasA. A second sensor designed to detect elastases is responsive to recombinant neutrophil elastase and secreted proteases from bacterial strains.
Findings: In mice infected with *P. aeruginosa*, nanoparticle formulations of these protease sensors—termed activity-based nanosensors (ABNs)—detect infections and monitor bacterial clearance from the lungs over time. Additionally, ABNs differentiate between appropriate and ineffective antibiotic treatments acutely, within hours after the initiation of therapy.
Interpretation: These findings demonstrate how activity measurements of disease-associated proteases can provide a noninvasive window into the dynamic process of bacterial infection and resolution, offering an opportunity for detecting, monitoring, and characterizing lung infections.
Fund: National Cancer Institute, National Institute of Environmental Health Sciences, National Institutes of Health, National Science Foundation Graduate Research Fellowship Program, and Howard Hughes Medical Institute.

1. Introduction

The prevalence of bacterial pneumonias, particularly in the context of decreasing efficacy of commonplace antibacterial agents, has emerged as a substantial threat to human health [1,2]. Our ability to robustly classify and monitor such infections has also lagged [3,4]. Early effective treatment is critical for decreasing the morbidity and mortality associated with pneumonia [5,6], though use of antibiotics that are inappropriate, unnecessary, or ineffective increases morbidity and promotes the development of antimicrobial resistance [3,7–9]. Following the initiation of antibiotic therapy, monitoring patients for drug efficacy is critical in deciding whether to continue, modify, or halt an antibiotic regimen [3,5,7]. Conventional monitoring techniques rely on nonspecific or slow measures, such as imaging the site of disease, measuring general markers of inflammation, or laboratory cultures of patient specimens, most of which are unable to identify patients for whom alternate therapeutics would be beneficial, and also fail to distinguish effective treatments from those that are inappropriate in a timely manner [10,11]. Existing molecular diagnostics for bacterial infections often rely on the measurement of a large and complex set of genes in blood samples, and thus may not capture the underlying pathogenesis quickly and in broadly applicable ways [12,13]. As such, simple diagnostic tools are urgently needed for the identification and characterization of bacterial pneumonias and their responses to treatment.

* Corresponding author at: 500 Main Street, 76-453, Cambridge, MA 02142, USA.
E-mail address: sbhatia@mit.edu (S.N. Bhatia).
[1] These authors contributed equally.

https://doi.org/10.1016/j.ebiom.2018.11.031

Research in context

Evidence before this study

Conventional approaches for the diagnosis and characterization of respiratory infections rely largely on radiographic imaging (*e.g.*, X-rays and CT scans), measurements of markers of inflammation (*e.g.*, C-reactive protein and erythrocyte sedimentation rate), and laboratory culture of sputum samples. Recent efforts to develop specific diagnostic tests to identify and categorize lung infections have utilized gene expression analyses of blood samples to generate classifier sets of genes that differentiate healthy from infected patients, as well those bearing bacterial infections from those with viral infections. These classifications require the measurement of numerous gene transcripts within blood samples, a process that can be costly and inaccessible. Additional efforts to diagnose bacterial lung disease have focused on activity measurements of proteases involved in the immune response to infection. These previous studies from our group have utilized sensors for common immune proteases, and thus lack specificity for bacterial infection over other sources of inflammation.

Added value of this study

In this work, we have designed nanoparticle sensors for protease activity that are responsive to both host- and pathogen-derived proteases. In this way, we can use noninvasive methods to monitor the lung microenvironment for both bacterial persistence and the immune response to the pathogen. This provides a robust diagnostic method with an ELISA-based readout of an exogenous urinary reporter molecule, allowing for rapid and affordable disease identification and monitoring.

Implications of all the available evidence

The capability to rapidly identify bacterial pneumonias and to monitor their treatment has great clinical relevance, particularly in an era of emerging antimicrobial resistance. The nanosensors described here offer rapid diagnosis of bacterial lung infections by measuring disease-associated protease activity, and allow for characterization of antibiotic treatment response soon after the initiation of therapy. The technology utilized here is additionally compatible with various point-of-care measurement techniques, such as lateral flow assays, offering a step towards an affordable, rapid, and broadly-deployable diagnostic tool.

Proteases are intricately involved in the development of and response to bacterial infections, and therefore offer an attractive route for diagnosis [14–16]. The human host response to pathogenic bacteria is highly proteolytically dependent, involving a number of proteases secreted by a range of innate immune cell types [17]. In addition, pathogen-derived proteases often act as virulence factors [14,18]. Previous work from our group has shown that protease-sensing nanoparticles, called activity-based nanosensors (ABNs) [19,20], can detect the inflammation associated with infection based on their cleavage by the metalloprotease, MMP9 [21]. However, while the measurement of activity of a target protease—rather than transcript levels or analyte concentrations—provides an amplified signal as well as a readout of the function of the biomarker, relying solely on MMP9-mediated detection hampers specificity of the sensor for infection, as MMP9 is associated with a variety of pathologies.

We reasoned that a set of protease targets and substrates designed to capture protease activity derived from both pathogen- and host-secreted enzymes would enable specific and robust monitoring of an infection. We first identified a pair of substrates that are susceptible to cleavage by proteases (including LasA and elastases such as neutrophil elastase) known to play a role in *P. aeruginosa* pneumonias and validated them *in vitro* across both lab and clinical strains. We subsequently barcoded this substrate set and coupled them to nanocarriers for simultaneous *in vivo* protease activity monitoring. We demonstrated the ability to detect the presence of a specific bacterial infection, monitor the response to prolonged antibiotic therapy, and also identify acutely efficacious *versus* ineffective antibiotic treatments. Characterization of this diagnostic tool by the generation of receiver operating characteristic (ROC) curves demonstrate its robust capability to identify infected *versus* healthy mice, as well as to acutely discriminate between insufficiently and successfully treated mice, as early as about one day following antibiotic administration.

2. Materials and methods

2.1. Bacterial pneumonia model and antibiotic treatment

All animal studies were approved by the Massachusetts Institute of Technology's Committee on Animal Care and were completed in accordance with the National Institutes of Health Guide for the Care and Use of Laboratory Animals. For infection studies, 5–7 week old female CD-1 mice were innoculated intratracheally with 1.25×10^6 CFU of *P. aeruginosa* strain PA01 in 50 μL of PBS. Bacteria were cultured overnight in LB broth, then subcultured and grown to log phase (OD600 ≈ 0.5). Bacteria were pelleted, washed with sterile PBS, and then resuspended to the requisite concentration for intratracheal administration. Mice were administered buprenorphine and meloxicam several hours after infection. For antibiotic treatment studies, mice were injected intraperitoneally with 40 mg/kg ciprofloxacin or 30 mg/kg doxycycline twice per day for up to six days.

2.2. Histochemistry of tissue sections

Animals were perfused with PBS followed by 10% formalin solution. The lungs were resected and fixed in formalin before paraffin embedding and sectioning. For gross histological evaluation of inflammation, lung sections were stained with hematoxylin and eosin. For immunofluorescent visualization of bacteria and neutrophils, lungs were stained with anti-pseudomonas (Abcam, RRID:AB_1270071, 1:500) or anti-neutrophil (Abcam, RRID:AB_303154, 1:500) antibodies. Appropriately labeled secondary antibodies (Invitrogen) were used to detect primary antibodies. Fluorescence images were acquired on a Perkin Elmer Pannoramic250. Quantification of neutrophil signal was completed by capturing 3–5 representative fields from each stained lung section and counting positive cells. Quantification of pseudomonas signal was completed by capturing 3–5 representative fields from each stained lung section and measuring total positive area after uniform thresholding of each single-channel fluorescence image (ImageJ).

2.3. Synthesis of peptides and NPs

All peptides were synthesized by CPC Scientific, Inc. For *in vitro* studies, intramolecularly quenched peptides were used by flanking the cleavable sequence with a FAM fluorophore and Dabcyl quencher. *In vivo* protease sensitive substrates were synthesized to contain a urinary reporter comprised of a protease resistant D-stereoisomer of Glutamate-Fibrinopeptide B with one of three ligand handles that could be captured by an antibody. Sequences are listed in Fig. 1b.

For *in vivo* studies, ABNs were synthesized by conjugating peptides to commercially-available multivalent 8-arm 40 kDa PEG-MAL (Jenkem). Excess of cysteine-terminated peptides were added to sterile-filtered PEG and reacted overnight. Unreacted peptide was removed using spin filters (Millipore, MWCO = 10 kDa). Based on prior

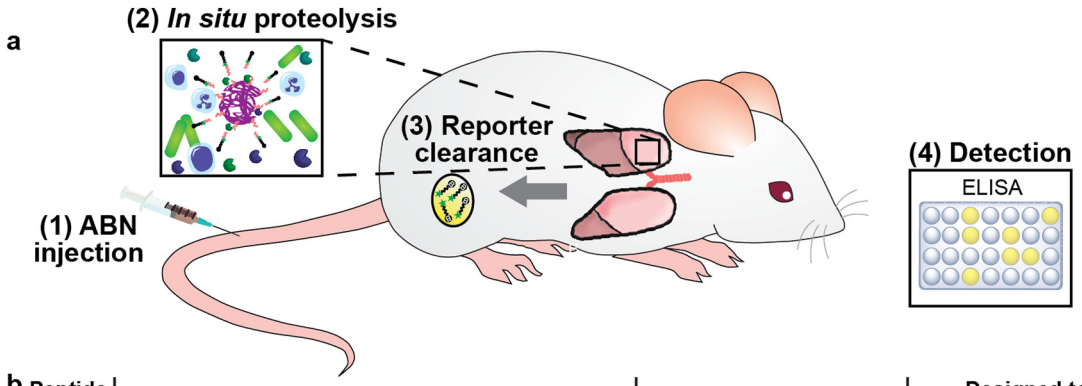

b

Peptide Name	Sequence	Readout	Designed to be responsive to
LAS-Q	Dabcyl-GLGGGAG(KFAM)-NH_2	Fluorescence dequenching of 5FAM	*P. aeruginosa* LasA
LAS-E	***Biotin***-eGvndneeGffsar(K***AF488***)GGLGGGAGC-NH_2	ELISA for AF488 and Biotin	
ELA-Q	Dabcyl-GAAFAG(KFAM)-NH_2	Fluorescence dequenching of 5FAM	Elastases (including neutrophil elastase)
ELA-E	***Biotin***-eGvndneeGffsar(K***FAM***)GGAAFAGC-NH_2	ELISA for FAM and Biotin	

Sequence Legend

Fluorophore LAS substrate ELA substrate Urinary reporter Coupling to PEG

Quencher Molecular spacers ***ELISA ligand handles*** lower case = D stereoisomer

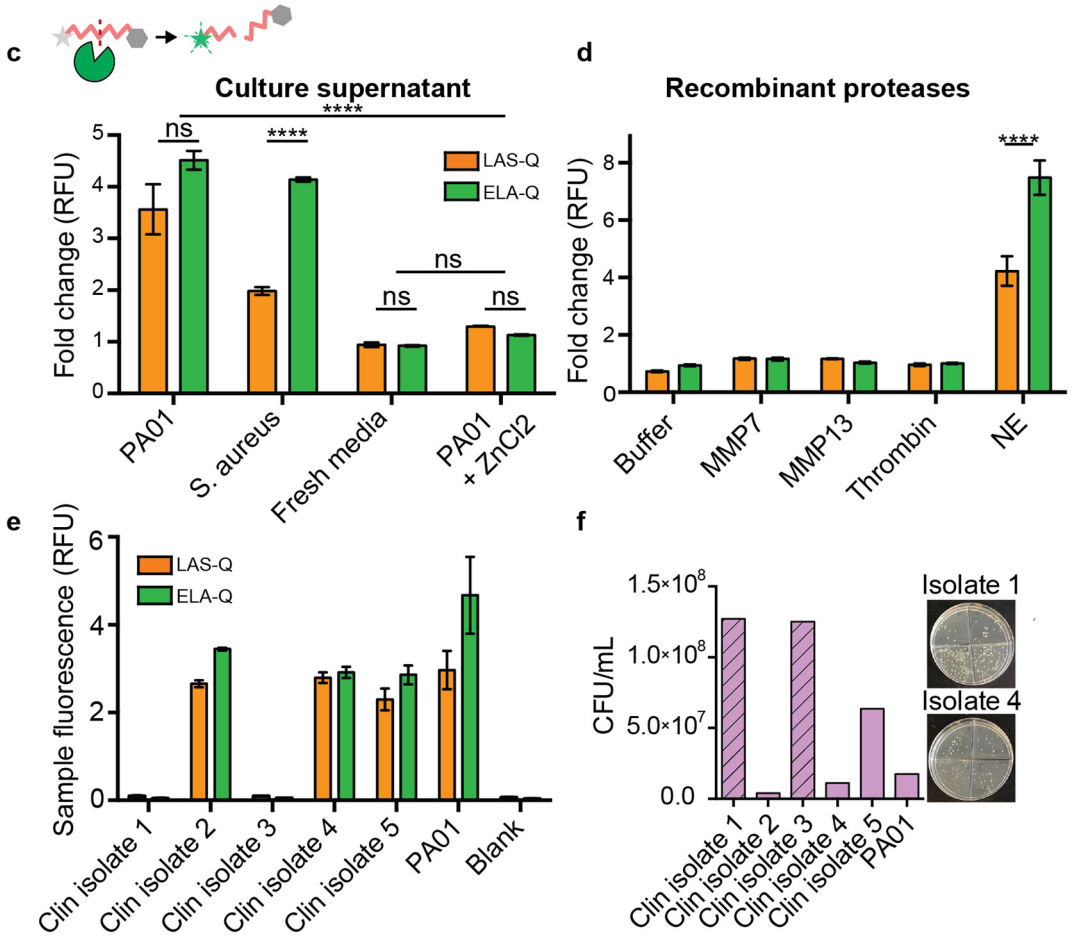

analysis of similar ABNs by RP-HPLC [22], we expect eight peptides per nanoparticle core, though this precise stoichimetry was not evaluated explicitly. Nanoparticles were stored in PBS at 4 °C. Peptide concentrations were quantified by absorbance (Tecan) to determine the ABN dose to be administered. Nanoparticles with this same PEG backbone with similar peptides conjugated to their surfaces have previously been characterized by dynamic light scattering (DLS) measurements and transmission electron microscopy (TEM), showing diameters around 10 nm and stability in PBS and serum over a range of temperatures [21,23].

2.4. In vitro substrate cleavage assays

Supernatant from PA01 and *S. aureus* were collected and added to substrates in 384 well plates and dequenching of FAM was monitored at 37 °C (Tecan). Fluorescence change at 30 min was reported. For recombinant protease assays, enzyme was added to the substrates in enzyme-specific buffer (MMP7 & 9 buffer: 50 mM Tris, 150 mM NaCl, 5 mM $CaCl_2$, 1 μM $ZnCl_2$, pH 7.5; Thrombin: PBS; NE: 100 mM HEPES, 500 mM NaCl, 0.05% Tween 20) in a 384 well plate for time-lapse fluorimetry to measure dequenching at 37 °C (Tecan).

2.5. Western blot of bacterial supernatants

Supernatants from PA01 and clinical isolate strains were collected from overnight cultures by centrifugation. 1 mL of supernatant or fresh media control was added to 250 μL of 50% trichloroacetic acid, then incubated for 15 min on ice to precipitate protein. Protein precipitates were collected by centrifugation, washed, and dried, then resuspended in LDS sample buffer (Invitrogen) with DTT. Samples were run on a 4–12% bis-tris gel (Invitrogen) along with 50 ng of recombinant LasA protein (MyBioSource) as a positive control, transferred to PVDF transfer membrane (Thermo Scientific). The membrane was blocked with 5% milk and blotted with HRP-conjugated anti-LasA (MyBioSource, RRID:AB_2750831, 1:10000), and visualized with SuperSignal West Pico PLUS chemiluminescent substrate (Thermo Scientific).

2.6. Stapholysis assay of bacterial supernatants

Supernatants from PA01 and clinical isolate strains were collected from overnight cultures by centrifugation. *S. aureus* was cultured overnight then subcultured in fresh LB and grown up to mid-log phase. *S. aureus* was then diluted 1:4 into each of the *P. aeruginosa* culture supernatants and grown for six hours, with aliquots taken and plated onto LB agar at various timepoints for CFU quantification.

2.7. In vivo assay for protease activity

At each timepoint, 200 μL of nanosensor cocktail were injected at a concentration of 1 μM per peptide in sterile PBS *via* the tail vein. After nanoparticle injection, mice were placed in custom housing with a 96-well plate base for urine collection. After one hour, their bladders were voided to collect between 100 and 200 μL of urine.

2.8. ELISA to quantify urinary reporters

Sandwich ELISAs were performed as previously described [24]. Briefly, capture antibodies (anti-fluorescein, GeneTex, RRID:AB_370572; anti-DNP, Invitrogen, RRID:AB_221552; and anti-AF488, Invitrogen, RRID:AB_221544) were coated onto Bacti plates (Thermo). Plates were washed and blocked and diluted urine (1000 to 10000-fold in PBS) was added. Detection was performed using NeutrAvidin-HRP (Pierce) and addition of Ultra-TMB as the substrate for HRP. After quenching with HCl, absorbace at 450 nm was measured. Concentration was calculated based on a standard curve ladder of peptide reporters liberated from the injected dose of ABNs, diluted from 1 μM starting concentration to 1 nM and below.

2.9. Clinical isolates

P. aeruginosa strains isolated from de-identified clinical samples were generously provided by Dr. Deborah Hung, MD, PhD (Massachusetts General Hospital). Cultures of each were grown in LB broth overnight, then were subcultured in fresh LB and each strain grown to OD-matched mid log phase (OD600~0.5). Supernatants were collected by centrifugation and substrate cleavage was monitored as described above.

2.10. Statistical and ROC analyses

All statistical analyses and receiver operating characteristic analyses were performed in GraphPad (Prism 6.0). Details of statistical tests are provided in the legend of each figure.

3. Results

3.1. Protease substrates respond to host and bacterial proteases in vitro

To develop ABNs for the diagnosis and monitoring of *Pseudomonas aeruginosa* infection, we identified candidate proteases upregulated at sites of infection as well as those produced by the pathogen, itself. Based on the robust neutrophil and macrophage recruitment response to bacterial infection [25], as well as the production of an elastase by *P. aeruginosa* [26], we first designed a candidate substrate responsive to elastase activity, including neutrophil elastase cleavage [27,28]. Additionally, we designed a substrate for the *P. aeruginosa* protease LasA, a virulence factor known to be secreted by strain PA01 [28–30]. After testing the candidate substrates for their cleavage specificity *in vitro*, we conjugated them to nanoparticle cores to form ABNs. By administering these LasA- or elastase-sensitive ABNs to infected mice, we predict that this tool will enable interrogation of proteolytic activity within the lung, and result in the cleavage-dependent liberation of small reporter fragments that are then able to clear *via* the kidneys and concentrate in the urine, in contrast with nanoparticle-bound reporter molecules that are too large to pass through the urinary filter (Fig. 1a). The reporters are designed to permit subsequent signal detection *via* ELISA and/or fluorescence for diagnosis of infection. To this end, each substrate was formulated for ELISA readout *via* ligand-encoded reporters by including a biotin distal to the protease-cleavable sequence (LAS-E and ELA-E) or were alternatively formulated for fluorescence measurement (LAS-Q and ELA-Q) by flanking the protease-cleavable sequence with a fluorophore-quencher FRET pair (Fig. 1b).

We tested the specificity of LAS and ELA for *P. aeruginosa* cleavage by collecting supernatants from PA01 or *Staphylococcus aureus* cultures and incubating them with FRET-paired substrates LAS-Q and ELA-Q in 384 well plates. We observed significant increases in fluorescence signal after cleavage of ELA-Q by proteases from both bacterial supernatants, but greater selectivity for cleavage of LAS-Q by PA01 (Fig. 1c). This pattern likely stems from *S. aureus* also secreting an analogous elastase that could cleave ELA-Q, yet this bacterial strain does not express a protease with function similar to LasA [31,32]. Addition of $ZnCl_2$ to PA01 supernatant suppressed the cleavage signal of both LAS-Q and ELA-Q, supporting the interpretation that the observed signal generation arises due to proteolytic cleavage, as $ZnCl_2$ has previously been shown to

Fig. 1. Diagnostic protease substrates respond to bacterial and host proteases *in vitro*. (a) Overview of activity-based nanosensor (ABN) platform for the detection of infection-associated proteases. Multiplexed ABNs are injected intravenously into mice [1] and encounter host and bacterial proteases *in situ*, which liberate stable peptide reporter molecules [2]. These small reporters are cleared by the kidneys and concentrated in the urine [3], where they are quantified by ELISA [4]. (b) Design of substrates against pathogen and host proteases. (c) Supernatants from PA01 or *Staphylococcus aureus* cultures were collected and incubated with FRET-paired substrates (LAS-Q and ELA-Q), alongside fresh media or PA01 supernatant supplemented with ZnCl2, and cleavage was monitored by fluorescence signal. Data are presented as relative fold change before and after incubation. (d) The same substrates assayed in (c) (LAS-Q and ELA-Q) were incubated with various disease-associated recombinant proteases including neutrophil elastase (NE), and examined for the reversal of FRET-quenched fluorescent signal. (e) Supernatants from *P. aeruginosa* clinical isolate strains and PA01 were collected and incubated with LAS-Q and ELA-Q substrates and cleavage was monitored by fluorescence signal, as in (c). (f) Colony forming units (CFU) present in lasA-sensitive *S. aureus* cultures grown in the presence of supernatants from clinical isolates and PA01 after six hours in culture. Striped bars indicate which clinical isolates produced supernatants that do not cleave ELA-Q and LAS-Q sensors. (****$P < 0.0001$; 2way ANOVA with Sidak's multiple comparisons test; n = 3 for each condition)

inhibit the cleavage activity of LasA [33] (Fig. 1c). By Michaelis-Menten type analysis, we confirmed that the ELA substrate was more potently cleaved by proteases over a range of concentrations (Fig. S1; V_{max} = 4.36 nM/min, K_m = 4.85 μM for LAS-Q; and V_{max} = 26.0 nM/min, K_m = 5.24 μM for ELA-Q). To investigate whether the LAS and ELA substrates are also susceptible to cleavage by host proteases, we incubated each with recombinant mouse proteases. Both substrates resist cleavage by MMP7, MMP13, and thrombin, but ELA-Q and – to a lesser extent, LAS-Q – are each cleaved by neutrophil elastase (NE, Fig. 1d). Together, these results suggest that our substrates should be cleaved by *P. aeruginosa*-derived proteases (LAS and ELA), and also yield a signal mediated by a host's immune response to the infection (ELA), and thus we anticipate that the LAS substrate signal should exhibit greater specificity for bacterial protease cleavage.

Once we observed that the two peptide substrates were cleaved when exposed to the supernatant of PA01 lab strain bacteria, we sought to test whether the candidate sensors also exhibit sensitivity to proteases produced by samples of *P. aeruginosa* obtained from infected patients. We collected supernatant from cultures of five clinical isolate strains and incubated them with LAS-Q and ELA-Q. We observed significant cleavage of both substrates by three of the five strains (Fig. 1e).

After observing that the sensors were not responsive to two of the five clinical isolate strains, we hypothesized that there might be a range of LasA protein secretion or activation between the bacterial samples. Given that LasA activity is known to mediate lysis of staphylococci [34], we first tested whether we observed a correlation between the capacity to mediate nanosensor substrate cleavage and anti-*Staphylococcus aureus* activity among these clinical isolates. We collected supernatants from PA01 and the five clinical isolates and grew *S. aureus* in cultures containing those supernatants and monitored bacterial growth. We observed suppression of *S. aureus* growth by PA01 supernatant (86% decrease) and supernatants from clinical isolates 2, 4, and 5 (97%, 91%, and 50%, respectively) relative to clinical isolates 1 and 3 (Fig. 1f). Next, to test whether LasA protein was being secreted by the clinical isolate strains we performed a Western blot on supernatant protein. This analysis found that the non-cleaving strains lacked LasA in their supernatant, whereas supernatant from the substrate-cleaving strains contained substantial levels of LasA protein (Fig. S2), supporting our hypothesis that cleavage of the LAS-Q sensor *in vitro* is detectable only in the presence of LasA protease activity.

3.2. ABNs detect P. aeruginosa infection in vivo

Next, we used an intratracheal instillation model of bacterial pneumonia with lab strain PA01, as it shows the highest cleavage of our sensors *in vitro*, demonstrates consistent infection dynamics in mice, and allows for robust comparison between experiments, to evaluate the ability of these ABNs to detect and monitor *P. aeruginosa* lung infection *in vivo* [21,35]. We coupled peptide substrates to 40 kDa 8-arm PEG-MAL *via* terminal cysteines on each peptide to generate ABNs for use *in vivo* [21,23]. Each substrate is barcoded with an independent ligand and a biotin on a stable urinary reporter peptide that can be measured by a sandwich ELISA after proteolysis of the substrate, release of the reporter, and clearance into the urine [24,36] (Fig. 2a, Fig. S3). The selection of a pair of distinct, ligand-encoded reporters enables simultaneous administration of the two nanosensors. We injected ABNs intravenously 24 h after initiation of the infection and collected urine one hour later. Characterization of the ligand-encoded reporters present in the urine indicated that each can be detected at the picomolar level —far more sensitively than is required based on the typical reporter concentration we observe in the urine—by ELISA (Fig. 2b). ELISAs for LAS-E and ELA-E reporters showed significant increases in each (1.8-fold and 2.6-fold, respectively) after initiation of infection relative to pre-infection measurements, and all but one individual mouse showed an increase in signal for both reporters after initiation of infection (Fig. 2c). To characterize the sensitivity and specificity of these ABNs for differentiating infected from healthy mice, we constructed receiver operating characteristic (ROC) curves, which demonstrate that LAS and ELA sensors are individually able to distinguish infected from healthy mice based on their urinary reporter signal (AUCs of 0.86 and 1.00 respectively; Fig. 2d).

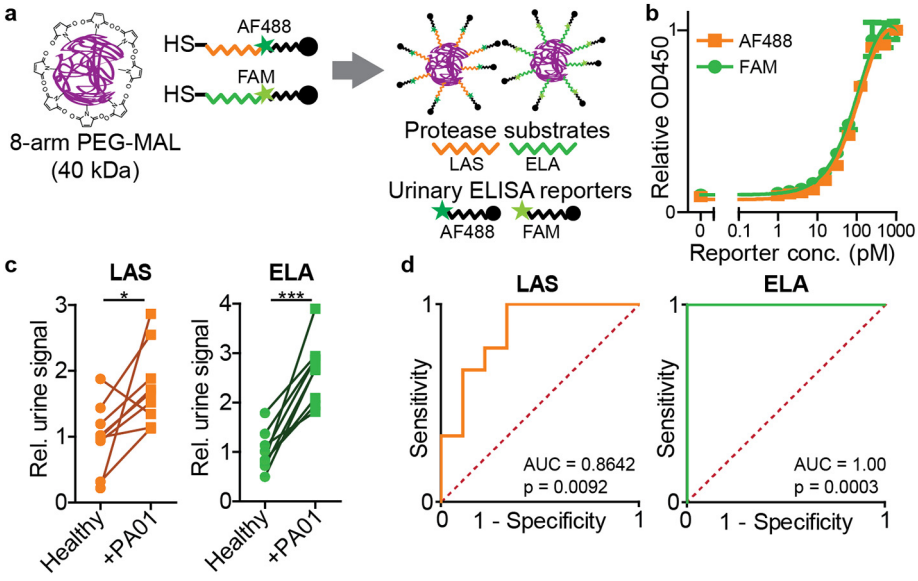

Fig. 2. LAS and ELA ABNs are able to detect *P. aeruginosa* infection *in vivo*. (a) Cysteine-terminated peptides barcoded with ligand-encoded urinary reporters were coupled to 8-arm PEG-MAL. Each substrate is uniquely barcoded with one of two ligands (dark/light green stars) and a biotin (black closed circles). (b) Characterization of ELISA measurements of AF488 liberated from cleaved LAS-E and FAM liberated from cleaved ELA-E after incubation with their respective specific proteases. (c) LAS and ELA reporter urine signal from healthy and subsequently PA01-infected mice administered ABNs intravenously 24 h post infection. Signal is normalized in each case to the mean healthy urine signal. Connectors indicate paired measurements in the same mice (LAS $p = 0.0281$, ELA $p = 0.0001$; two-tailed paired *t*-test, n = 9 mice). (d) ROC curves determining the diagnostic accuracy of the assay for each substrate's ability to distinguish infected from healthy urine signal. An AUC of 1 represents a perfect classifier, and an AUC of 0.5 (dashed red line of identity) represents a random classifier. *P* values relative to a random classifier.

3.3. ABNs detect acute resolution of bacterial infection after antibiotic therapy

To evaluate whether our ABNs could be used to monitor acute clearance of infection, we instilled PA01 intratracheally into mice, administered the pair of ABNs the following day to confirm/set a baseline for infection in each individual, and then initiated antibiotic treatment with ciprofloxacin, a commonly used broad spectrum antibiotic with activity against gram-negative bacteria, including PA01 [37]. We repeated the diagnostic ABN injection and urine collection seven days post-infection (with an interceding course of antibiotic treatment) to determine whether our substrates could monitor recovery from infection following effective antibiotic treatment (Fig. 3a). After ciprofloxacin treatment, LAS urine signal returned to baseline, though ELA remained elevated (1.2-fold and 2.2-fold above baseline, respectively; Fig. 3b-c). Constructing ROC curves to test whether the sensors could distinguish between healthy and infected mice again showed robust capability to diagnose infection with both LAS and ELA (AUC 0.92 and 1.00, respectively) when administered prior to drug treatment. However, ROC curve analysis of the urine signal after treatment (relative to infected mice prior to treatment) indicated that only the LAS ABN could identify successful treatment (AUC 0.88).

The persisting elevation in ELA urine signal at day seven meant ELA ABNs were unable to measure treatment success, and suggested there may be remnant inflammation within the lungs of treated mice even after antibiotic therapy and resolution of infection (Fig. 3c). To test whether inflammation remained after antibiotic therapy, we performed histological and immunofluorescence analysis of lung sections from infected and treated mice. As expected based on urinary readouts, histology and immunofluorescent staining of lung sections show residual

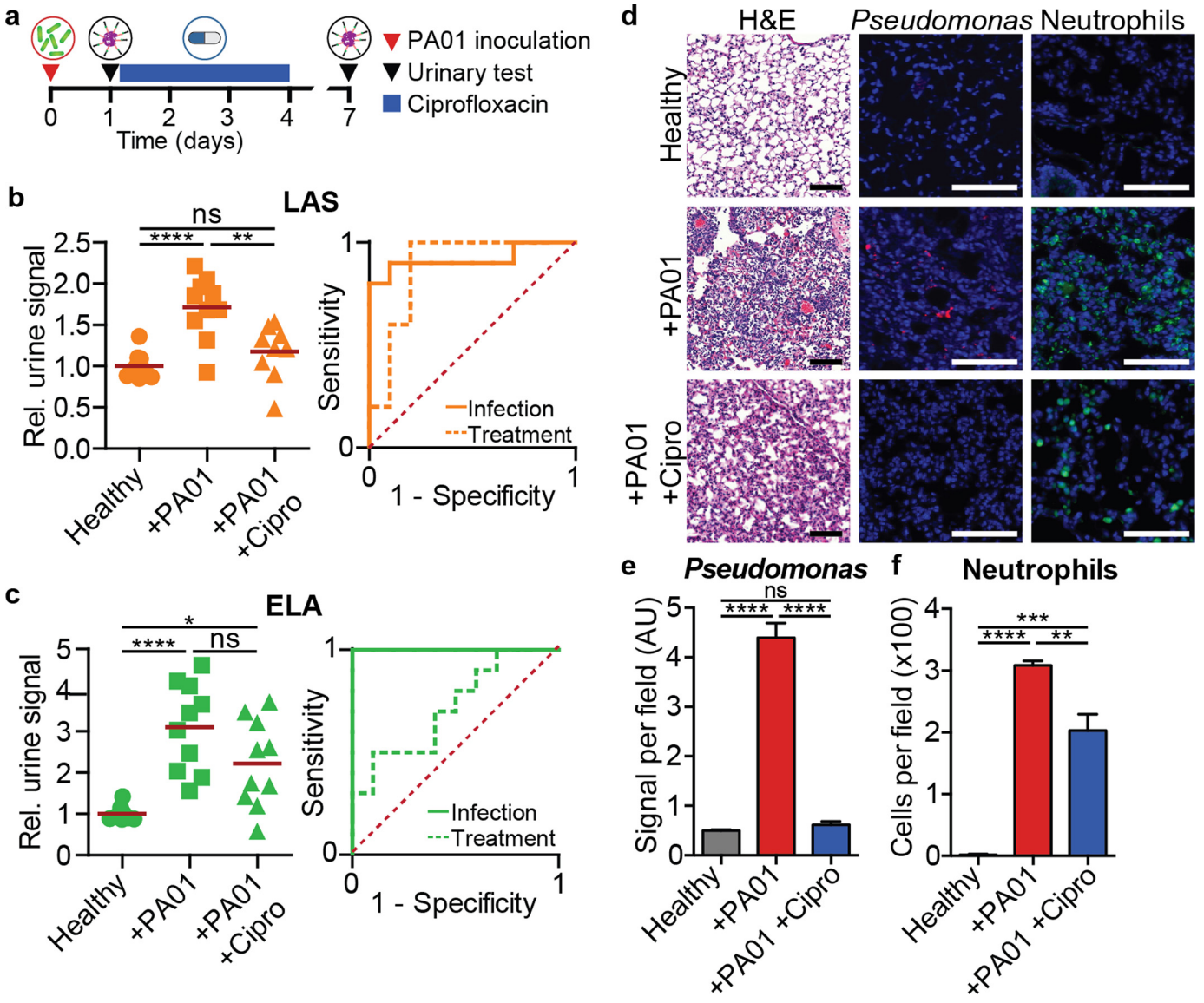

Fig. 3. ABNs detect acute resolution of bacterial infections after antibiotic therapy. (a) Experimental overview: PA01-infected mice are injected with nanosensors to assess the baseline levels of reporter signal, then started on a four day course of ciprofloxacin treatment. Seven days following infection, diagnostic injections and urine collections are repeated to monitor for nanosensor readout. (b-c) LAS-E (b) and ELA-E (c) urine signal from infected mice (+PA01) and subsequently treated with ciprofloxacin (+PA01 + Cipro) relative to healthy control measurements and ROC curves for each substrate to distinguish infected from healthy (Infection, solid curves; ELA AUC = 1.00, $p < 0.001$ from random classifier, LAS AUC = 0.92, $p = 0.002$ from random classifier) or ciprofloxacin treated from pre-treatment signal (Treatment, dashed curves; ELA AUC = 0.72, $p = 0.096$ from random classifier, LAS AUC = 0.88, $p = 0.004$ from random classifier). (d) Gross histology (left) and immunofluorescence staining for *Pseudomonas* (red, middle) and neutrophils (green, right) in lung sections from healthy, acutely infected (24 h), and ciprofloxacin-treated mice. (e-f) Quantification of *Pseudomonas* (e) and neutrophil (f) immunofluorescence staining in lung sections from healthy, infected (+PA01), and ciprofloxacin-treated infected (+PA01 + Cipro) mice. (****$P < 0.0001$, ***$P < 0.001$, **$P < 0.01$, *$P < 0.05$; 1way ANOVA with Tukey's multiple comparisons test; n = 10 mice (b-c), n = 3–4 mice, 3 representative fields per mouse (e-f)).

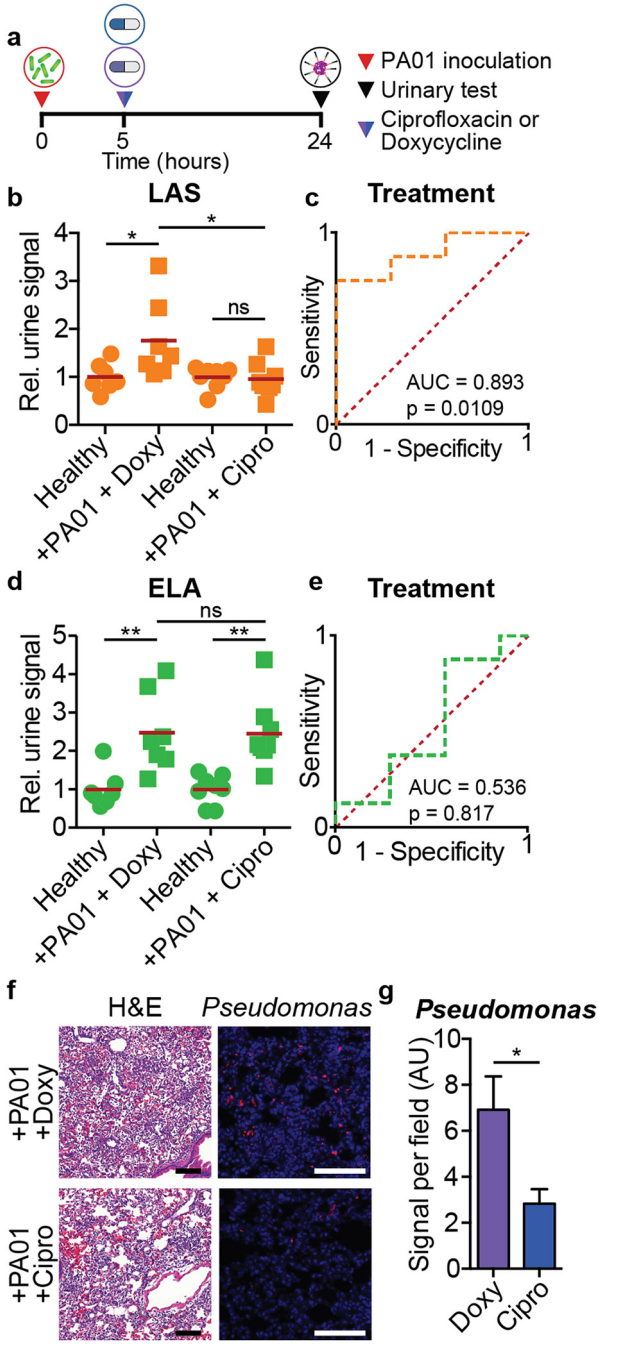

Fig. 4. ABNs identify acute drug sensitivity *versus* resistance in developing infections. (a) Experimental overview: mice are infected with PA01, then treatment with either ciprofloxacin or doxycycline is initiated five hours post-infection. Nanosensors are injected and urine is collected 24 h post-infection. (b) Relative LAS urine signal before infection and after initiation of ciprofloxacin or doxycycline treatment. (c) ROC curve for LAS signal differentiating between effective and ineffective treatment (doxycycline-treated *vs* ciprofloxacin-treated). (d) Relative ELA urine signal before infection and after initiation of ciprofloxacin or doxycycline treatment. (e) ROC curve for ELA signal differentiating between effective and ineffective treatment. (f) Lung histology (left, H&E) and immunofluorescence staining for *Pseudomonas* (red, right) of doxycycline and ciprofloxacin-treated mice 24 h post-infection, after 19 h of antibiotic therapy. (g) Quantification of *Pseudomonas* immunofluorescence signal in lung sections from doxycycline- and ciprofloxacin-treated mice. (**$P < 0.01$, *$P < 0.05$; 1way ANOVA with Tukey's multiple comparisons test, n = 7–8 mice (b,d); *P*-values relative to a random classifier (c,e); two-tailed Student's *t*-test, n = 6–9 fields from 2 to 4 mice per group (g)).

inflammation and elevated presence of neutrophils after ciprofloxacin treatment, but no *Pseudomonas* (Fig. 3d). Quantification of immunofluorescence signal from *Pseudomonas* showed significantly higher signal in lungs of infected mice relative to uninfected or ciprofloxacin-treated mice (7–9-fold), but no significant difference in signal between uninfected and ciprofloxacin-treated mice with resolved infections (Fig. 3e). Additionally, quantification of neutrophils within the lungs of uninfected, infected, or infected and ciprofloxacin-treated mice showed robust increase in neutrophil numbers within infected mice relative to uninfected mice, as well as an ~30% decrease in neutrophil count in lungs of mice after antibiotic treatment, still well above the uninfected baseline (Fig. 3f). These results suggest the persisting presence of immune cell-derived proteases drives cleavage of the ELA-E substrate, but the absence of PA01 LasA to cleave LAS-E, supporting the hypothesis that urinary measurements reflect features of the lung microenvironment post-infection. The robust diagnostic capability of ELA to identify infection but poor ability to monitor treatment, paired with the robust ability for LAS to specifically monitor treatment highlights the importance of multiplexing and measuring both host and pathogen factors.

3.4. Acute administration of ABNs differentiates successful versus insufficient antibiotic therapies

Individual responses to antimicrobial treatment can be highly variable, dependent upon the strain of pathogen and the presence of antibiotic resistance, and current clinical tests take 24–72 h to identify antibiotic susceptibility [3]. In addition, current clinical tests used to visualize lung infections (*e.g.*, chest X-ray and computed tomography) are often unable to distinguish active infections from those that have been adequately treated until several weeks after antibiotic therapy is complete, because the airspace opacifications characteristic of pneumonia remain apparent on routine radiography screens [10]. Therefore, we sought to evaluate the ability of our infection-tracking ABNs to identify successful *versus* insufficient treatment on an acute time-scale, shortly after therapeutic initiation. Only five hours after establishing lung infections with PA01, we initiated antibiotic treatment with either ciprofloxacin (efficacious against *P. aeruginosa*) or doxycycline (ineffective against gram-negative bacteria including *P. aeruginosa*) (Fig. 4a). The following day, we administered multiplexed LAS-E and ELA-E ABNs and collected urine. ELISAs for protease-liberated reporters in the urine detected elevated LAS signal in the urine of doxycycline-treated mice but not in those treated with ciprofloxacin, whereas the ELA signal was robustly elevated in both antibiotic treatment groups relative to healthy controls. Comparing the urine signal from the two treatment groups, we see that LAS signal is significantly lower in ciprofloxacin-treated mice than in doxycycline-treated mice, whereas ELA signal between the two groups is not significantly different (Fig. 4b and d). Constructing ROC curves to query whether the sensors could detect effective treatment (comparing doxycycline to ciprofloxacin treatment) reveals that LAS does characterize acute drug sensitivity *versus* resistance (Fig. 4c, AUC = 0.893), whereas ELA is unable to differentiate treatment groups (Fig. 4e, AUC = 0.536). This data is in line with the timeline in which an infection is expected to activate an innate immune response, in that neutrophil infiltration occurs on the order of a few hours in mice [38]. To assay whether we observed lingering inflammatory cells in the infected, antibiotic treated animals, we performed histology and immunofluorescence analyses in lung sections and observed marked lung inflammation and elevated neutrophils in both doxycycline- and ciprofloxacin-treated mice, consistent with elevated ELA signal in both (Fig. 4f). However, a significantly lower *Pseudomonas* immunofluorescent signal was present in the lungs of ciprofloxacin-treated mice compared to the doxycycline-treated group (~60%

decrease, Fig. 4g). The persistent *Pseudomonas* immunostaining observed following ciprofloxacin treatment might be derived from residual *Pseudomonas* antigens remaining from lysed bacteria that had not yet been cleared by the immune system. Alternatively, the reduced LAS sensor reading in these treated mice could reflect a suppression of LasA secretion from bacteria as they are killed by the potent antibiotic. Thus, ABNs are able to noninvasively report on the status of the infection and lung microenvironment, and taken together, these data support the potential to use ABNs to test the performance of antibiotics *in vivo*, without requiring sputum cultures or the reliance on slowly evolving clinical metrics such as fever or malaise.

4. Discussion

Here, we developed an activity-based nanosensor set for the detection of *P. aeruginosa* pneumonia, a disease associated with high morbidity and mortality. Together, our data demonstrate that the engineered ABN platform is deployable to the context of infection, both for the specific identification of *P. aeruginosa* lung infections and for the monitoring of their treatment. The strategy to measure both host- and pathogen-derived protease activity provides a noninvasive window into the lung microenvironment over the course of disease and resolution. This approach facilitates the rapid identification of infection and the monitoring of bacterial clearance following antibiotic treatment. In this study, we utilized an intratracheal instillation method for the development of *P. aeruginosa* infections, which relies on an inoculation of a large bolus of bacteria for infection to take hold. As such, one potential limitation of this work is the limit of detection for bacterial burden within the lung. We have shown detection of pneumonia with burdens of $>10^6$ CFU of bacteria disseminated throughout the lung, but established mouse models are limited in their ability to generate focal infections that are more directly analogous to human disease, or those with lower bacterial burdens. We expect the limit of bacterial detection could be lowered by direct pulmonary administration of ABNs, such as by nebulization of the particles [39].

An exciting aspect of the urine-based nanosensor detection platform is that it can be readily interfaced with paper tests or lateral flow assays as the analytical readout, which can be imaged using a cell phone camera [21,24]. This adaptation could enable at-home or out-patient monitoring, as well as use in low resource settings. Utilizing paper- or lateral flow-based readouts could also decrease the time between diagnostic administration and final measurement quantification by eliminating the serial steps required for traditional ELISA-based analyte measurements.

While the pair of nanosensors described here is able to detect PA01 infection, it may not cover all *P. aeruginosa* strains and may not perfectly differentiate *P. aeruginosa* infections from those caused by other bacterial species. For example, our screen of five clinical isolates highlights that not all strains of *P. aeruginosa* secrete detectable levels of LasA, and our supernatant cleavage assays demonstrated some measurable cleavage of the LAS sensor by *S. aureus* supernatant, though to a less extent than *P. aeruginosa* supernatant. Higher level multiplexing would overcome these limitations, such as by adding detectors for other pathogen-derived proteases, including the *P. aeruginosa* virulence factors LepA, Protease IV, and AprA. Doing so would be expected to improve detection of various *P. aeruginosa* strains and also enhance the ability to differentiate between *P. aeruginosa* infections and those caused by other bacterial species. We have previously shown that we can multiplex >15 substrates simultaneously in the context of prostate cancer [22], and would therefore anticipate being able to add sensors for many more bacterial and/or immune system proteases. This greater multiplexing could also facilitate the application of ABNs to robustly classify viral from bacterial infections, which represents a challenging stumbling block in the diagnosis of childhood pneumonia [12], among other at-risk demographics.

Collectively, the work described here demonstrates the capacity to use protease activity measurements to identify, monitor, and characterize bacterial lung infections. Notably, this method could also be adapted *via* the design of alternative peptide substrates for different host- and pathogen-derived proteases to be applicable to a wide range of clinical pathologies. Through the co-administration of a pair of peptide substrates, ABNs succeeded in differentiating between healthy and infected mice, and also monitored the course of disease after treatment, thereby distinguishing between appropriate and ineffective antibiotic regimens soon after therapeutic administration. These results offer a proof-of-principle demonstration that could be adapted for new applications, such as to identify distinct disease etiologies, to monitor severity of disease, and to illuminate and/or track an immune response during the course of an infection.

Funding sources

This study was supported in part by a Koch Institute Support Grant No. P30-CA14051 from the National Cancer Institute (Swanson Biotechnology Center), and a Core Center Grant P30-ES002109 from the National Institute of Environmental Health Sciences. This work was also supported in part by the National Institute of Allergy and Infectious Diseases of the National Institutes of Health (R01-AI132413). J.S.D. and C.G.B. thank the National Science Foundation Graduate Research Fellowship Program for support. S.N.B. is a Howard Hughes Medical Institute Investigator. Funding sources had no involvement in the study design; collection, analysis, and interpretation of data; in the writing of the paper; or in the decision to submit the paper for publication.

Declaration of interests

C.G.B., J.S.D., and S.N.B. are listed as inventors on a patent application related to this work. S.N.B. is a shareholder of and consultant to Glympse Bio.

Author contributions

C.G.B., J.S.D., R.T.K.A., H.E.F., and S.N.B. designed research; C.G.B., J.S.D., and R.T.K.A. performed research; C.G.B., J.S.D., and S.N.B. analyzed data; and C.G.B., J.S.D., H.E.F., and S.N.B. wrote the paper.

Acknowledgements

The authors thank the Koch Institute Swanson Biotechnology Center for technical support, specifically Kathleen Cormier in the Hope Babette Tang Histology Facility. We thank Dr. Ester Kwon for reagents and discussion, and Maria Ibrahim for technical assistance.

Appendix A. Supplementary data

Supplementary data to this article can be found online at https://doi.org/10.1016/j.ebiom.2018.11.031.

References

[1] Mizgerd JP. Acute lower respiratory tract infection. N Engl J Med 2008;358:716–27. https://doi.org/10.1056/NEJMra074111.
[2] Mizgerd JP. Lung infection - a public health priority. PLoS Med 2006;3:0155–8. https://doi.org/10.1371/journal.pmed.0030076.
[3] Caliendo AM, Gilbert DN, Ginocchio CC, Hanson KE, May L, Quinn TC, et al. Better tests, better care: Improved diagnostics for infectious diseases. Clin Infect Dis 2013;57:S139–70. https://doi.org/10.1093/cid/cit578.
[4] Bartlett JG. Diagnostic tests for agents of community-acquired pneumonia. Clin Infect Dis 2011;52:S296–304. https://doi.org/10.1093/cid/cir045.
[5] Iregui M, Ward S, Sherman G, Fraser VJ, Kollef MH. Clinical importance of delays in the initiation of appropriate antibiotic treatment for ventilator-associated pneumonia. Chest 2002;122:262–8. https://doi.org/10.1378/chest.122.1.262.

[6] Bartlett JG, Breiman RF, Mandell LA, File TM. Community-acquired pneumonia in adults: Guidelines for management. Clin Infect Dis 1998;26:811–38. https://doi.org/10.1086/513953.
[7] Dupont H, Mentec H, Sollet JP, Bleichner G. Impact of appropriateness of initial antibiotic therapy on the outcome of ventilator-associated pneumonia. Intensive Care Med 2001;27:355–62. https://doi.org/10.1007/s001340000640.
[8] Leroy O, Meybeck A, D'Escrivan T, Devos P, Kipnis E, Georges H. Impact of adequacy of initial antimicrobial therapy on the prognosis of patients with ventilator-associated pneumonia. Intensive Care Med 2003;29:2170–3. https://doi.org/10.1007/s00134-003-1990-x.
[9] Kollef MH, Sherman G, Ward S, Fraser VJ. Inadequate Antimicrobial Treatment of Infections. Chest 1999;115:462–74. https://doi.org/10.1378/chest.115.2.462.
[10] Bruns AHW, Oosterheert JJ, El Moussaoui R, Opmeer BC, Hoepelman AIM, Prins JM. Pneumonia recovery; discrepancies in perspectives of the radiologist, physician and patient. J Gen Intern Med 2010;25:203–6. https://doi.org/10.1007/s11606-009-1182-7.
[11] Coelho L, Póvoa P, Almeida E, Fernandes A, Mealha R, Moreira P, et al. Usefulness of C-reactive protein in monitoring the severe community-acquired pneumonia clinical course. Crit Care 2007;11:R92. https://doi.org/10.1186/cc6105.
[12] Sweeney TE, Wong HR, Khatri P. Robust classification of bacterial and viral infections via integrated host gene expression diagnostics. Sci Transl Med 2016;8:346ra91. https://doi.org/10.1126/scitranslmed.aaf7165.
[13] Zumla A, Al-Tawfiq JA, Enne VI, Kidd M, Drosten C, Breuer J, et al. Rapid point of care diagnostic tests for viral and bacterial respiratory tract infections-needs, advances, and future prospects. Lancet Infect Dis 2014;14:1123–35. https://doi.org/10.1016/S1473-3099(14)70827-8.
[14] Matsumoto K. Role of bacterial proteases in pseudomonal and serratial keratitis. Biol Chem 2004;385:1007–16. https://doi.org/10.1515/BC.2004.131.
[15] Parks WC, Wilson CL, López-Boado YS. Matrix metalloproteinases as modulators of inflammation and innate immunity. Nat Rev Immunol 2004;4:617–29. https://doi.org/10.1038/nri1418.
[16] Iwasaki A, Medzhitov R. Control of adaptive immunity by the innate immune system. Nat Immunol 2015;16:343–53. https://doi.org/10.1038/ni.3123.
[17] Wilkinson TS, Conway Morris A, Kefala K, O'Kane CM, Moore NR, Booth NA, et al. Ventilator-associated pneumonia is characterized by excessive release of neutrophil proteases in the lung. Chest 2012;142:1425–32. https://doi.org/10.1378/chest.11-3273.
[18] Potempa J, Pike RN. Corruption of innate immunity by bacterial proteases. J Innate Immun 2009;1:70–87. https://doi.org/10.1159/000181144.
[19] Kwong GA, von Maltzahn G, Murugappan G, Abudayyeh O, Mo S, Papayannopoulos IA, et al. Mass-encoded synthetic biomarkers for multiplexed urinary monitoring of disease. Nat Biotechnol 2013;31:63–70. https://doi.org/10.1038/nbt.2464.
[20] Kwon EJ, Dudani JS, Bhatia SN. Ultrasensitive tumour-penetrating nanosensors of protease activity. Nat Biomed Eng 2017;1:0054. https://doi.org/10.1038/s41551-017-0054.
[21] Dudani JS, Buss CG, Akana RTK, Kwong GA, Bhatia SN. Sustained-release synthetic biomarkers for monitoring thrombosis and inflammation using point-of-care compatible readouts. Adv Funct Mater 2016;26:2919–28. https://doi.org/10.1002/adfm.201505142.
[22] Dudani JS, Ibrahim M, Kirkpatrick J, Warren AD, Bhatia SN. Classification of prostate cancer using a protease activity nanosensor library. Proc Natl Acad Sci U S A 2018;115:8954–9. https://doi.org/10.1073/pnas.1805337115.
[23] Kwong GA, Dudani JS, Carrodeguas E, Mazumdar EV, Zekavat SM, Bhatia SN. Mathematical framework for activity-based cancer biomarkers. Proc Natl Acad Sci 2015;112:12627–32. https://doi.org/10.1073/pnas.1506925112.
[24] Warren AD, Kwong G a, Wood DK, Lin KY, Bhatia SN. Point-of-care diagnostics for noncommunicable diseases using synthetic urinary biomarkers and paper microfluidics. Proc Natl Acad Sci U S A 2014;111:3671–6. https://doi.org/10.1073/pnas.1314651111.
[25] Mayadas TN, Cullere X, Lowell CA. The Multifaceted Functions of Neutrophils. Annu Rev Pathol Mech Dis 2014;9:181–218. https://doi.org/10.1146/annurev-pathol-020712-164023.
[26] Kamath S, Kapatral V, Chakrabarty AM. Cellular function of elastase in Pseudomonas aeruginosa: Role in the cleavage of nucleoside diphosphate kinase and in alginate synthesis. Mol Microbiol 1998;30:933–41. https://doi.org/10.1046/j.1365-2958.1998.01121.x.
[27] Castillo MJ, Nakajima K, Zimmerman M, Powers JC. Sensitive substrates for human leukocyte and porcine pancreatic elastase: A study of the merits of various chromophoric and fluorogenic leaving groups in assays for serine proteases. Anal Biochem 1979;99:53–64. https://doi.org/10.1016/0003-2697(79)90043-5.
[28] Elston C, Wallach J, Saulnier J. New continuous and specific fluorometric assays for Pseudomonas aeruginosa elastase and LasA protease. Anal Biochem 2007;368:87–94. https://doi.org/10.1016/j.ab.2007.04.041.
[29] Kaman WE, El Arkoubi-El Arkoubi N, Roffel S, Endtz HP, van Belkum A, Bikker FJ, et al. Evaluation of a FRET-peptide substrate to predict virulence in pseudomonas aeruginosa. PLoS One 2013;8:e81428. https://doi.org/10.1371/journal.pone.0081428.
[30] Spencer J, Murphy LM, Conners R, Sessions RB, Gamblin SJ. Crystal structure of the LasA virulence factor from pseudomonas aeruginosa: Substrate specificity and mechanism of M23 metallopeptidases. J Mol Biol 2010;396:908–23. https://doi.org/10.1016/j.jmb.2009.12.021.
[31] Shaw L. The role and regulation of the extracellular proteases of *Staphylococcus aureus*. Microbiology 2004;150:217–28. https://doi.org/10.1099/mic.0.26634-0.
[32] Potempa J, Dubin A, Korzus G, Travis J. Degradation of elastin by a cysteine proteinase from *Staphylococcus aureus*. J Biol Chem 1988;263:2664–7.
[33] Kessler E, Safrin M, Abrams WR, Rosenbloom J, Ohman DE. Inhibitors and specificity of Pseudomonas aeruginosa LasA. J Biol Chem 1997;272:9884–9. https://doi.org/10.1074/jbc.272.15.9884.
[34] Kessler E, Safrin M, Olson JC, Ohman DE. Secreted LasA of Pseudomonas aeruginosa is a staphylolytic protease. J Biol Chem 1993;268:7503–8.
[35] Kwon EJ, Skalak M, Bertucci A, Braun G, Ricci F, Ruoslahti E, et al. Porous silicon nanoparticle delivery of tandem peptide anti-infectives for the treatment of Pseudomonas aeruginosa lung infections. Adv Mater 2017;29:1701527. https://doi.org/10.1002/adma.201701527.
[36] Lin KY, Lo JH, Consul N, Kwong GA, Bhatia SN. Self-titrating anticoagulant nanocomplexes that restore homeostatic regulation of the coagulation cascade. ACS Nano 2014;8:8776–85. https://doi.org/10.1021/nn501129q.
[37] Zeiler H-J, Grohe K. The in vitro and in vivo activity of ciprofloxacin. Ciprofloxacin. Wiesbaden: Vieweg+Teubner Verlag; 1986. p. 14–8. https://doi.org/10.1007/978-3-663-01930-5_3.
[38] Zhang P, Summer WR, Bagby GJ, Nelson S. Innate immunity and pulmonary host defense. Immunol Rev 2000;173:39–51. https://doi.org/10.1034/j.1600-065X.2000.917306.x.
[39] Patton JS, Byron PR. Inhaling medicines: Delivering drugs to the body through the lungs. Nat Rev Drug Discov 2007;6:67–74. https://doi.org/10.1038/nrd2153.